The Ebola Virus Glycoprotein and HIV-1 Vpu Employ Different Strategies to Counteract the Antiviral Factor Tetherin

Annika Kühl,[1] Carina Banning,[2] Andrea Marzi,[3] Jörg Votteler,[4] Imke Steffen,[1] Stephanie Bertram,[1] Ilona Glowacka,[1] Andreas Konrad,[5] Michael Stürzl,[5] Ju-Tao Guo,[6] Ulrich Schubert,[4] Heinz Feldmann,[3] Georg Behrens,[7] Michael Schindler,[2] and Stefan Pöhlmann[1,8]

[1]Institute of Virology, Hannover Medical School, [2]Heinrich Pette Institute – Leibniz Institute for Experimental Virology and Immunology, Hamburg, Germany; [3]Laboratory of Virology, Division of Intramural Research, NIAID, NIH, Rocky Mountain Laboratories, Hamilton, Montana; [4]Institute of Virology, and [5]Department of Surgery, Division of Molecular and Experimental Surgery, University of Erlangen Nuremberg, Germany; [6]Department of Microbiology and Immunology, Drexel University College of Medicine, Philadelphia, Pennsylvania; [7]Clinic for Immunology and Rheumatology, Hannover Medical School, and [8]Department of Infection Biology, German Primate Research Center, Göttingen, Germany

The antiviral protein tetherin/BST2/CD317/HM1.24 restricts cellular egress of human immunodeficiency virus (HIV) and of particles mimicking the Ebola virus (EBOV), a hemorrhagic fever virus. The HIV-1 viral protein U (Vpu) and the EBOV-glycoprotein (EBOV-GP) both inhibit tetherin. Here, we compared tetherin counteraction by EBOV-GP and Vpu. We found that EBOV-GP but not Vpu counteracted tetherin from different primate species, indicating that EBOV-GP and Vpu target tetherin differentially. Tetherin interacted with the GP2 subunit of EBOV-GP, which might encode the determinants for tetherin counteraction. Vpu reduced cell surface expression of tetherin while EBOV-GP did not, suggesting that both proteins employ different mechanisms to counteract tetherin. Finally, Marburg virus (MARV)–GP also inhibited tetherin and downregulated tetherin in a cell type–dependent fashion, indicating that tetherin antagonism depends on the cellular source of tetherin. Collectively, our results indicate that EBOV-GP counteracts tetherin by a novel mechanism and that tetherin inhibition is conserved between EBOV-GP and MARV-GP.

The interferon-α (IFNα)–inducible cellular protein tetherin is a novel human immunodeficiency virus (HIV) restriction factor, which inhibits the release of progeny virions from infected cells [1, 2]. The antiviral action of tetherin is counteracted by the HIV-1 accessory viral protein U (Vpu), which is required for efficient release of HIV-1 from tetherin-expressing cells [2]. Thus, tetherin might constitute a potent barrier against Vpu-deficient HIV-1, and the molecular mechanism underlying tetherin inhibition by Vpu might be a target for therapeutic inhibition [3].

Ebola virus (EBOV) and Marburg virus (MARV) are enveloped, negative-stranded RNA viruses that comprise the family *Filoviridae*. Outbreaks of filoviral hemorrhagic fever occur sporadically and unpredictably in central Africa [4]. The viral VP40 protein drives budding of progeny particles from infected cells [5], and the release of VP40-based virus-like particles (VLPs) was shown to be inhibited by tetherin [6, 7]. Tetherin-dependent inhibition of viral release was counteracted by the coexpression of the EBOV glycoprotein (GP) [8], indicating that EBOV, like HIV, is targeted by tetherin and has countermeasures available to ensure efficient viral release from tetherin-positive cells. In fact, several enveloped viruses, including retro-, arena-, filo-, and herpes viruses are inhibited by tetherin and evolved strategies to counteract tetherin's antiviral activity [6, 9–14].

Tetherin is a type II transmembrane protein that encodes an N-terminal transmembrane domain and

a C-terminal glycosylphosphatidylinositol anchor, and is thus able to span membranes twice [15]. This property is believed to be essential for tetherin's antiviral activity, since recent evidence suggests that tetherin is active as a parallel homodimer, which inserts 1 pair of membrane anchors into the cellular membrane and the other pair into the viral membrane [16], thereby tethering progeny particles to the cell surface [16–19]. Vpu was shown to downregulate tetherin from the cell surface [20, 21] and to target it for proteasomal [21, 22] or lysosomal [23] degradation, thereby preventing tetherin from accumulating at the site of viral budding. In contrast, it is at present unknown how EBOV-GP counteracts tetherin.

Here, we show that the inhibition of tetherin is conserved between the GPs of EBOV and MARV, and might involve the interaction of tetherin with the GP2 subunit of GP. In addition, we demonstrate that EBOV-GP can counteract tetherin without downregulating its cell surface expression, indicating that EBOV-GP has evolved a novel mechanism to antagonize tetherin.

METHODS

Cell Culture and Transfection
Human embryonic kidney 293T and HeLa cells were cultured in Dulbecco's modified Eagle's medium (DMEM) supplemented with 10% fetal calf serum (FCS) and antibiotics. A 293 cell line expressing tetherin in a tetracycline-inducible manner was generated as previously described [24]. All cells were grown at 37°C in humidified atmosphere containing 5% CO_2. The 293T cells were transfected by the calcium phosphate method; HeLa cells were transfected with Lipofectamine 2000 (Invitrogen).

Expression Vectors
Plasmids encoding HIV-1 Gag (p55) [25], Vpu [26], ZEBOV-GP (*Zaire ebolavirus*, Mayinga strain), SEBOV-GP (*Sudan ebolavirus*, Boniface strain), ZEBOV-GP with C-terminal V5-tag, and MARV-GP (*Lake Victoria Marburgvirus*, Musoke strain) were described previously [27, 28]. BEBOV-GP (Bundibugyo virus, GenBank FJ217161) was amplified from viral RNA and cloned into plasmid pCAGGS. The plasmid encoding Kaposi's sarcoma–associated herpes virus (KSHV) K5-protein was previously described [29]. The generation of pCR3.1 plasmids encoding tetherin from human and nonhuman primates was described elsewhere [30, 31]. The expression plasmids for Vpu-YFP and tetherin-CFP fusion proteins were described previously [32, 33], and plasmids encoding EBOV-GP-YFP fusion proteins were generated by the same cloning strategy [32]. All PCR-derived inserts were sequenced to confirm sequence identity.

Antibodies
A previously described monoclonal antibody against human tetherin was used for fluorescence-activated cell sorting (FACS) and for immunofluorescence analyses [34]. For FACS experiments, a Cy5-coupled secondary antibody (Dianova) was employed; isotype-matched controls were from R&D Systems. A fluoresceinisothiocyanate (FITC)-labeled anti-V5 antibody (Invitrogen) and a secondary Rhodamine RedX goat antimouse antibody (Dianova) were used for immunofluorescence. Rabbit antihuman tetherin serum [35] was used for Western blot. For immunoprecipitation studies, monoclonal anti-GFP (Roche) and M2-anti-FLAG-HRP antibodies (Sigma) were used. An anti-p24 hybridoma supernatant (183-H12-5C) was used for p55-Gag detection by Western blot. Goat antimouse- and antirabbit-HRP antibodies (Dianova) were used for protein detection by Western blot.

VLP Release Assay
The 293T cells seeded in 6-well plates were cotransfected with plasmids encoding Gag or VP40, tetherin, and either Vpu or filovirus GPs or KSHV-K5 or cotransfected with empty vector. Forty-eight hours after transfection, supernatants were cleared from debris and centrifuged through 20% sucrose at 21 100 g. The pelleted VLPs, and producer cells harvested in parallel, were lysed in SDS-loading buffer and analyzed by Western blot.

PNGase F Digestion of Cell Lysates
Cells were resuspended in TNE buffer and subsequently incubated in glycoprotein denaturing buffer at 95°C for 15 minutes. Thereafter, NP-40, G7 reaction buffer, and PNGase F (New England Biolabs) were added, and the samples further incubated for 1 hour at 37°C before mixing with 2 x SDS-loading buffer.

Flow Cytometric Analysis of Tetherin Expression
For analysis of tetherin surface expression, 293T cells seeded in 6-well plates were cotransfected with plasmids encoding tetherin and the specified viral proteins or cotransfected with empty plasmid. Alternatively, tetherin expression in 293T cells was induced by IFNα (Sigma) before transfection and further maintained in the presence of IFNα. Finally, HeLa cells, which express endogenous tetherin, were transfected with plasmids encoding viral proteins or empty vector. After 48 hours, the cells were detached, stained, and analyzed by flow cytometry using a Cytomics FC500 flow cytometer (Beckman Coulter).

Immunofluorescence
HeLa cells transfected with plasmids encoding Vpu-YFP fusion protein or ZEBOV-GP C-terminally tagged with V5 or control vector were fixed with 4% paraformaldehyde and incubated with 50 mM ammonium chloride for quenching. Samples were permeabilized with 0.2% Triton-X 100 and subsequently blocked with 3% bovine serum albumin (BSA) followed by incubation with primary and secondary antibodies. Nuclei were counterstained with 4′,6-diamidino-2-phenylindole (DAPI). Images were acquired with a Zeiss Observer Z1 microscope.

FACS-Based FRET and Confocal Microscopy

FACS–fluorescence resonance energy transfer (FRET) measurements were performed as described previously [32]. Briefly, transfected 293T cells were assayed for FACS-FRET analysis in a FACSAria cytometer (BD Bioscience). For enhanced cyan fluorescent protein (ECFP) and FRET measurements, cells were excited with a 405-nm laser and ECFP emission was collected with a standard 450/40 filter, while FRET was measured with 529/24 filter (Semrock). For enhanced yellow fluorescent protein (EYFP) measurement, cells were excited with a 488-nm laser and emission was collected with a 529/24 filter (Semrock). At least 1000 ECFP/EYFP–positive cells were analyzed for FRET. To assess subcellular localization via confocal microscopy, cells were grown on coverslips and mounted on microscope slides. Imaging was done with a Zeiss LSM510 Meta microscope. Maximum intensity projection and 3D surface reconstruction of stacks were done with the Bitplane Imaris software (version 6.4).

Zaire Ebolavirus Infection

The 293 cells, seeded in 12-well plates and tetracycline-induced to express tetherin, were infected with ZEBOV (Mayinga strain) at a multiplicity of infection (MOI) of 0.01. After 1 hour, the inoculum was removed and the cells cultured in fresh medium supplemented with tetracycline. After 24 hours, culture supernatants and cells were collected, lysed in 4% sodium dodecyl sulfate (SDS) loading buffer, boiled for 15 min, and removed from the biosafety level 4 (BSL4) laboratory for Western blot analysis in BSL2, according to standard operating protocols. All ZEBOV experiments were performed in the high-containment facility at the Integrated Research Facility, Division of Intramural Research (DIR), National Institute of Allergy and Infectious Diseases (NIAID), National Institutes of Health (NIH), in Hamilton, Montana, USA.

RESULTS

Tetherin Counteraction Is Conserved Between the Glycoproteins of Ebola and Marburg Virus

The GP of the EBOV species Zaire (ZEBOV) was previously shown to inhibit tetherin [8]. We asked if the ability to counteract tetherin was conserved between the GPs of different EBOV species and MARV-GP. For this, we transiently coexpressed HIV-1 Gag (which drives the release of VLPs), human tetherin, and filovirus GPs in 293T cells and determined Gag levels in cell lysates and cellular supernatants. In the absence of tetherin, coexpression of filovirus GPs or HIV-1 Vpu had no effect on Gag levels in cell lysates and culture supernatants (Figure 1A). When tetherin was coexpressed with Gag, the amount of Gag in cellular supernatants (but not in cell lysates) was markedly reduced, and the inhibition of Gag release was rescued by Vpu and ZEBOV-GP (Figure 1A), in agreement with

previous studies [1, 8]. The GP of the *Sudan ebolavirus* species (SEBOV), the GP of the proposed species *Bundibugyo ebolavirus* (BEBOV), as well as MARV-GP were also able to counteract tetherin (Figures 1A and 1B).

Ebola Virus Glycoproteins But Not Vpu Are Active Against Tetherin Alleles From Nonhuman Primate Species

We next investigated if EBOV-GPs were able to counteract tetherin alleles from rhesus macaque, African green monkey, and gorilla, all of which develop severe disease upon EBOV infection [36, 37]. ZEBOV-GP and SEBOV-GP, which were active against human tetherin, also counteracted the tetherin alleles from all primate species tested (Figure 1A), and similar results were obtained for MARV-GP and BEBOV-GP (data not shown). In contrast, Vpu was only active against gorilla tetherin (Figure 1A), as expected [10, 30, 31, 38]. Collectively, EBOV-GP and Vpu exhibit different activities against primate tetherin alleles and might thus target tetherin differently.

Ebola Virus Glycoproteins Counteract Endogenous Tetherin, and Tetherin Expression Modestly Reduces Release of *Zaire Ebolavirus*

ZEBOV-GP and SEBOV-GP as well as Vpu augmented the release of VLPs from HeLa cells (Figure 2A), which express endogenous tetherin (see below). A modest inhibition of ZEBOV release by high levels of tetherin would suggest that tetherin could restrict viral spread in vivo and might thereby force the virus to have appropriate defenses in place. To address this possibility, we employed replication-competent ZEBOV for infection of 293 cells expressing tetherin upon induction with tetracycline. Tetherin expression consistently resulted in a slight decrease in VP40 release into culture supernatants and a slight increase in VP40 levels in cell lysates (Figures 2B and 2C), indicating that tetherin was indeed able to diminish ZEBOV release under the conditions tested.

Tetherin Interacts With the GP2 Subunit of the *Zaire Ebolavirus* Glycoprotein

We next sought to investigate if EBOV-GP, like Vpu, interacts with tetherin. For this, we employed a previously described FACS-based FRET assay [32]. To measure FRET signals elicited upon ZEBOV-GP and tetherin contact, we employed a CFP-tetherin fusion construct [32, 39] and fused YFP to the C-terminus of ZEBOV-GP or to the C-terminus of the isolated ZEBOV-GP surface unit, GP1, and the isolated transmembrane unit, GP2, respectively. Analysis of 293T cells expressing a CFP-YFP fusion protein as a positive control revealed a robust FRET signal (Figure 3A), as expected [32]. In contrast, no appreciable FRET signal was detected upon coexpression of CFP-tetherin with C-terminally tagged ZEBOV-GP, GP1, or GP2 (Figure 3A). Confocal microscopy of transfected cells revealed that ZEBOV-GP-YFP was located in intracellular vesicles and at the plasma membrane, as expected, while GP1-YFP was diffusely distributed in
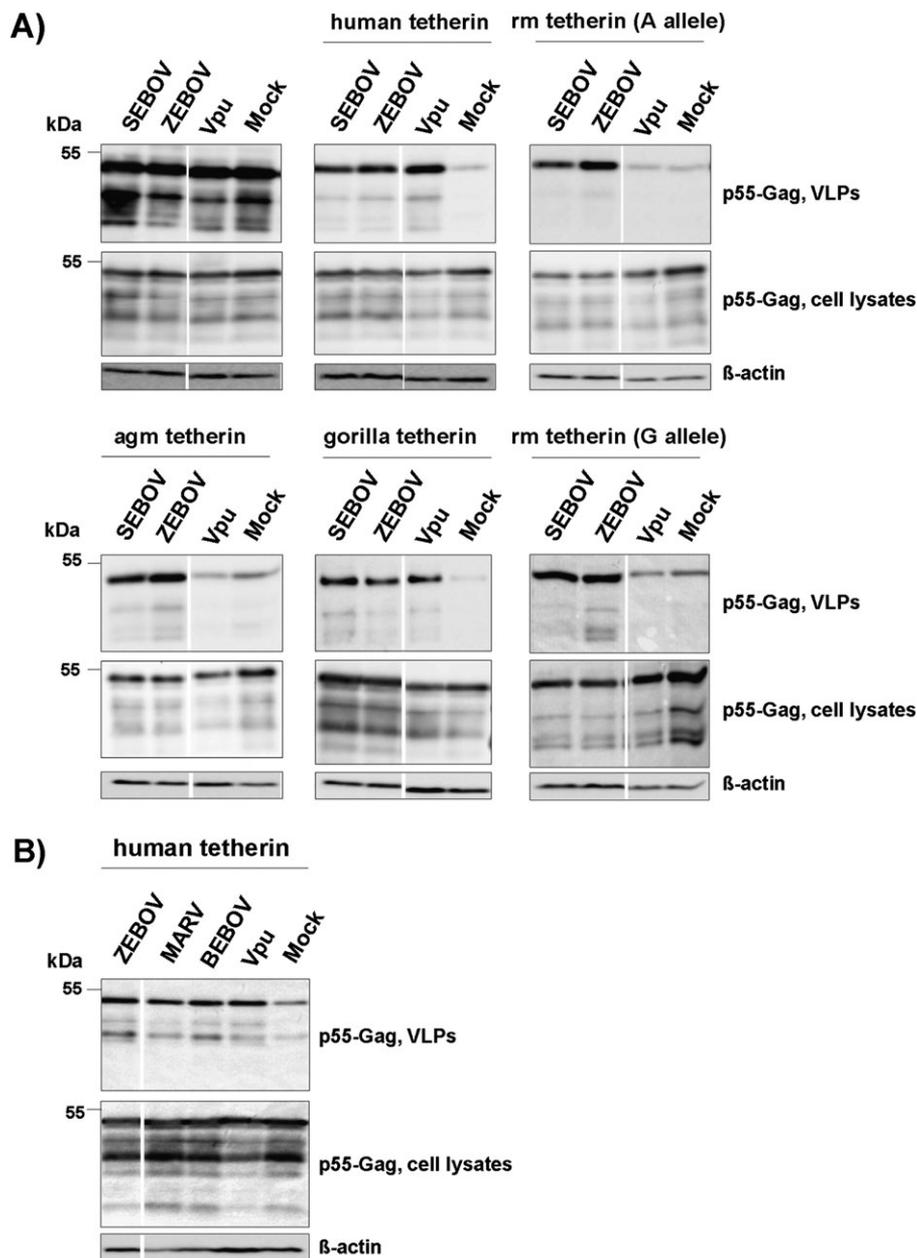
Figure 1. Counteraction of tetherin by Vpu but not the Ebola virus glycoprotein is species specific. *A*, Plasmids encoding HIV-1 p55 Gag and GPs from the indicated EBOV species or Vpu were cotransfected into 293T cells in the presence and absence of plasmids encoding tetherin derived from the indicated species. The presence of p55-Gag in cell lysates and supernatants was subsequently determined by Western blot. Detection of β-actin served as loading control. Similar results were obtained in 2 to 4 independent experiments. agm, African green monkey; rm, rhesus macaque. *B*, The experiment was conducted as in (*A*), but the anti-tetherin activity of ZEBOV-GP, MARV-GP, BEBOV-GP, and Vpu was tested. The results of representative single gels from which irrelevant lanes were excised are shown in (*A*) and (*B*).

cells and GP2-YFP was mainly detected in subcellular dot-like structures with a smaller proportion at the plasma membrane (Figure 3B). Upon coexpression of tetherin, ZEBOV-GP-YFP relocalized to some extent to intracellular structures with partial tetherin-colocalization (Figure 3C). In contrast to this, EBOV-GP1-YFP did not show pronounced tetherin-colocalization, whereas GP2 seemed to accumulate together with tetherin (Figure 3C). A 3D reconstruction of z-stacks and

maximum intensity projections revealed that GP2-YFP folds into pockets of a larger tetherin accumulation (Figure 3D, *upper panel*). Therefore, we considered the possibility that in our experimental setup, spatial constraints (particularly a separating cellular membrane) might impede detection of tetherin interactions with GP2 by FRET. To address this, we swapped the YFP-tag of GP2 to the N-terminus and indeed measured a robust FRET signal in 293T cells cotransfected with CFP-tetherin
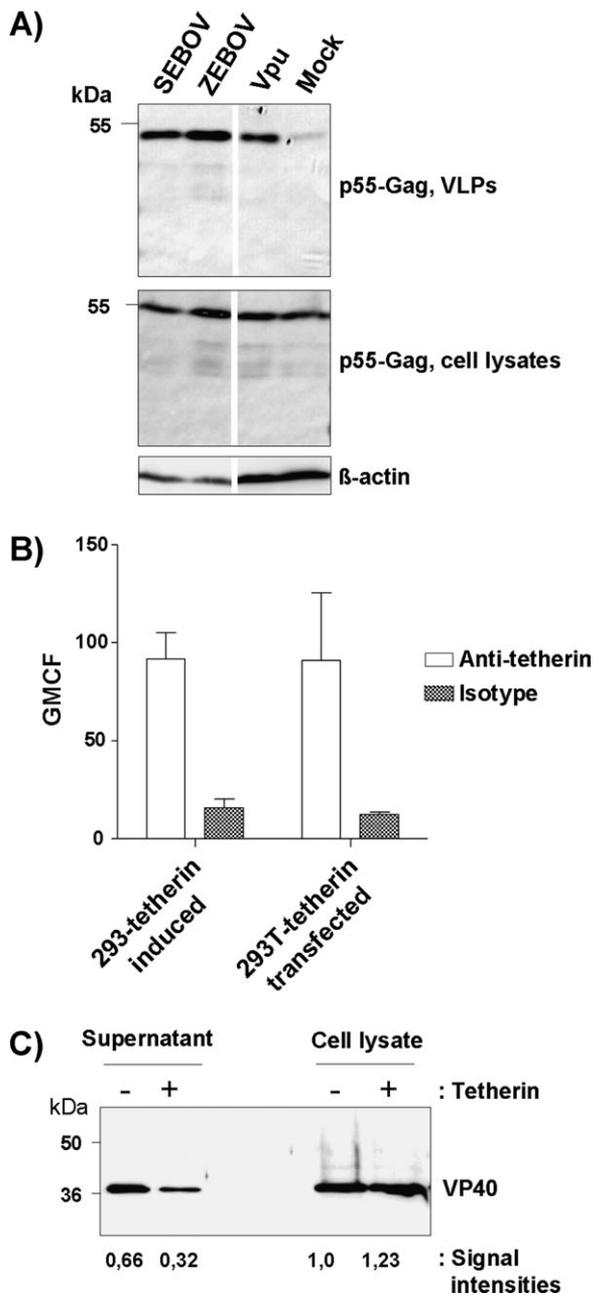
Figure 2. Evidence for an impact of tetherin on release of replication competent *Zaire ebolavirus*. *A*, The impact of EBOV-GPs on the release of p55-Gag from HeLa cells, which express endogenous tetherin (see Figure 4), was assessed via cotransfection of plasmids encoding HIV-1 p55-Gag and the GPs of the indicated EBOV species or Vpu. The results were confirmed in 2 independent experiments. *B*, Tetherin expression on transiently transfected 293T cells and on tetracycline-induced 293-tetherin cells was detected by flow cytometry. The average of 3 independent experiments is shown; error bars indicate standard error of the mean (SEM). *C*, Tetherin expression by 293-tetherin cells was induced by treatment with tetracycline, the cells infected with ZEBOV at a MOI of 0.01, washed, and VP40 present in culture supernatants and cell lysates detected by Western blot. The intensities of the signals measured by Western blot were quantified by Image J software and are shown relative to the signal measured for the lysates of uninduced cells. Similar results were obtained in an independent experiment and with 293T cells transiently expressing tetherin upon transfection.

(Figure 3A). As expected, the YFP-GP2 showed a more pronounced membrane staining, because the N-terminal YFP tag is on the extracellular site of the transmembrane protein (Figure 3B). Upon coexpression with tetherin, the YFP-GP2 fusion protein was found inside the cell and strongly colocalized with tetherin (Figures 3C and 3D, *lower panel*). Finally, we assessed if tetherin interactions with ZEBOV-GP2 could be demonstrated in a different experimental system. Coimmunoprecipitation studies revealed that tetherin was able to pull down ZEBOV-GP and ZEBOV-GP2 but not ZEBOV-GP1 (Figure 3E), supporting our conclusion that tetherin interacts with the GP2 subunit of ZEBOV-GP.

Differential Interference of Filovirus Glycoproteins and Vpu With Tetherin Expression

It was previously shown that Vpu and the K5 protein of KSHV negatively regulate tetherin expression [13, 21–23, 40]. We compared the impact of filovirus GPs, Vpu, and KSHV-K5 on tetherin expression in tetherin-transfected 293T cells, IFNα-induced 293T cells, and HeLa cells, which express endogenous tetherin. FACS analysis was utilized to quantify surface-expressed tetherin, while Western blot analysis was used to determine the total amount of tetherin. Expression of Vpu profoundly reduced total tetherin expression in transfected and IFNα-induced 293T cells (Figures 4A and 4B, *right panels*), and in the latter cells, the reduced expression of total tetherin translated into a marked reduction of surface-expressed tetherin (Figure 4B, *left panel*). In fact, the degree of tetherin downregulation when transiently expressed in transfected 293T cells was likely much more pronounced than suggested by the mock control in Figure 4A. Thus, tetherin surface expression was consistently higher in cells coexpressing the murine leukemia virus envelope protein (which does not antagonize tetherin [41]) compared with cells in the mock control, likely because of efficient sequestration of transcription factors by the empty plasmid used as mock control. Markedly diminished surface expression of tetherin was also observed in Vpu-transfected HeLa cells, but the decrease in surface tetherin levels was not paralleled by a marked decrease in total tetherin expression (Figure 4C, *right panel*), in agreement with previously reported findings [42].

In contrast to Vpu, expression of the EBOV-GPs had no impact on total tetherin expression (Figure 4, *right panel*) and did not (Figure 4A, *left panel*) or did only slightly (Figures 4B and 4C, *left panels*) reduce cell surface levels of tetherin. Similar observations were made for MARV-GP, except that downregulation of surface-expressed tetherin in IFNα-induced 293T cells was efficient (Figure 4, *left panel*). Finally, KSHV-K5 did not alter total tetherin expression under all conditions tested but efficiently reduced tetherin levels at the surface of HeLa cells (Figure 4C). In contrast, surface expression of tetherin in transfected and IFNα-induced 293T cells was not modulated by
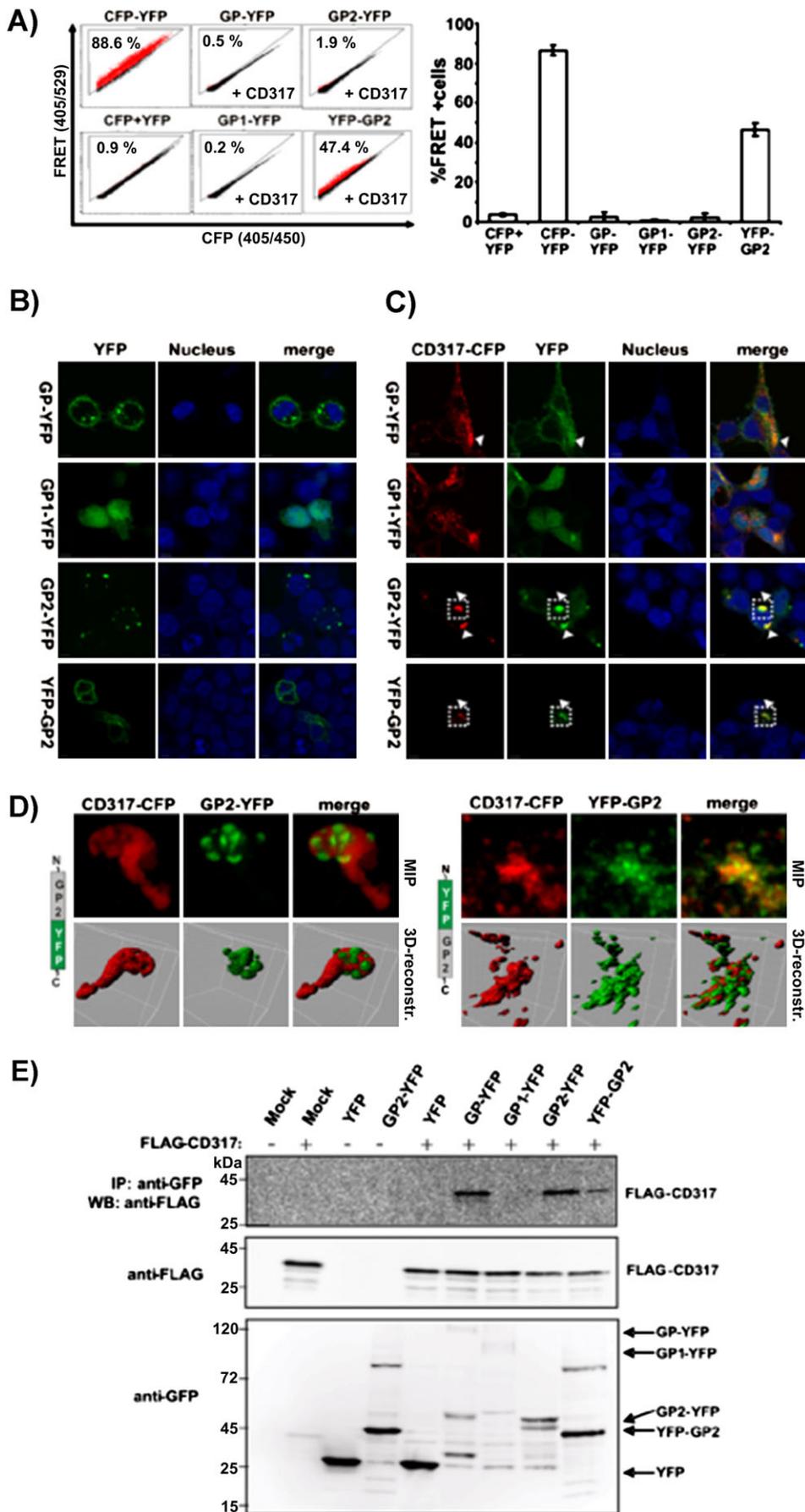
K5 (Figure 4, *left panel*). These results indicate that interference of viral defense proteins with tetherin expression is cell type–dependent and that the reduction of surface and total tetherin expression does not necessarily correlate.

Tetherin Glycosylation Depends on the Source of Cellular Tetherin

To explore potential reasons for the cell type dependence of tetherin antagonism, we asked if N-glycosylation of tetherin varied between cell lines. Western blot analysis revealed substantial size differences between tetherin in transfected 293T cells and tetherin in IFNα-induced 293T and HeLa cells (Figure 5); with signals ranging from 25–30 and 50–60 kDa corresponding to tetherin mono- and dimers, respectively. Digest of cell lysates with PNGase F, which removes all N-linked glycans, uniformly resulted in bands at approximately 20 and 40 kDa (Figure 5), which correspond to tetherin monomers and dimers, demonstrating that the differences in tetherin size observed for untreated cells were due to differential glycosylation, which might impact tetherin activity and sensitivity to counteraction by viral defense proteins.

Vpu But Not Ebola Virus Glycoprotein Induces Accumulation of Tetherin in Intracellular Compartments

Expression of Vpu efficiently reduced tetherin surface levels in HeLa cells, while expression of ZEBOV-GP did not (Figure 4). We sought to clarify if these proteins also had differential effects on the cellular localization of tetherin. Immunofluorescence analysis of ZEBOV-GP-transfected HeLa cells revealed that the presence of ZEBOV-GP had no marked effect on the cellular distribution of tetherin (Figure 6). In contrast, expression of Vpu fused to YFP caused a marked accumulation of tetherin in intracellular vesicles (Figure 6), as expected from previous work [1], indicating that Vpu but not ZEBOV-GP can modulate the intracellular localization of tetherin.

DISCUSSION

The HIV-1 Vpu protein and the EBOV-GP counteract the antiviral host cell protein tetherin. While multiple lines of evidence indicate that the blockade of tetherin is important for HIV-1 spread in patients [3], similar evidence is missing for EBOV. Conservation of tetherin antagonism between the GPs of different EBOV species and MARV would suggest biological relevance. Despite considerable sequence diversity—EBOV-GP and MARV-GP share only 28% amino acid identity—the GPs of all filoviruses tested here were able to counteract tetherin, indicating that tetherin antagonism might be important for efficient viral spread in infected primates.

Tetherin inhibits the release of VLPs driven by the HIV-1 Gag and the EBOV matrix protein VP40 [1, 6]. We compared the impact of EBOV-GP on Gag and VP40 release in the presence and absence of tetherin. Both ZEBOV-GP and SEBOV-GP promoted the release of VP40 particles but not Gag particles in the absence of tetherin (Figure 1 and Supplemental Figure 1), an observation that precluded the use of VP40 for the analysis of tetherin antagonism. Augmentation of VP40 release by ZE-BOV-GP is in agreement with results published by Licata and colleagues [43] but not with previous work by Kaletsky and colleagues [8]. The reasons for this discrepancy are at present unclear but might involve differences in ZEBOV-GP expression, processing, and maturation.

The observations that tetherin expression is inducible by IFNα [1] and that uninduced macrophages, important target cells of filoviruses [4], express endogenous tetherin [35, 39] suggest that tetherin could modulate filovirus infection in primates. Our data, particularly the finding that tetherin modestly reduced ZEBOV release from infected cells, lend further support to this hypothesis. A recent study that reported that expression of tetherin in 293 cells did not decrease ZEBOV spread [44] seems to argue against a role of tetherin in filovirus spread. However, a substantially higher MOI (0.5) was used in this study compared with our study (MOI = 0.01) and modest inhibitory effects of tetherin might have been missed.

The immediate strategy for viruses to counteract tetherin is to reduce tetherin expression, and several reports indicate that Vpu indeed decreases cell surface levels of tetherin [20–23, 42, 45]. Our results indicate that EBOV-GP, like Vpu, has the ability to interfere with tetherin surface expression (see Figure 4B). However, EBOV-GPs can clearly block tetherin by a mechanism other than downregulation since efficient tetherin counteraction in HeLa cells and particularly in transfected 293T cells was not paralleled by efficient reduction of tetherin expression at the plasma membrane, in agreement with recently published reports [41, 46]. While it cannot be excluded that moderate effects of EBOV-GPs on tetherin surface expression in HeLa cells were biologically meaningful, it is more likely that EBOV-GP interferes with the configuration or integrity of plasma membrane–inserted tetherin. In agreement with such

Figure 3. The GP2 subunit of the Ebola virus glycoprotein interacts with tetherin. *A*, FACS-based FRET analysis of 293T cells transfected with EBOV-GP-YFP fusion proteins and CFP-tetherin (CD317). Mean and SD are derived of 2 independent experiments with duplicate transfections. *B*, Confocal images of 293T cells transfected with the EBOV-GP-YFP fusion proteins only, or (*C*) cotransfected with CFP-CD317. *D*, Maximum intensity projection and 3D surface reconstruction of the cropped regions indicated in (*C*). CFP is shown in red and YFP in green. *E*, Coimmunoprecipitation of the GP2 subunit and tetherin. The 293T cells were transfected with EBOV-GP-YFP fusion proteins and FLAG-tagged tetherin. Anti-GFP antibody was used for immunoprecipitation, and anti-FLAG and anti-GFP antibodies for Western blot analysis of immunoprecipitates (top panel) and cell lysates (middle and bottom panels).
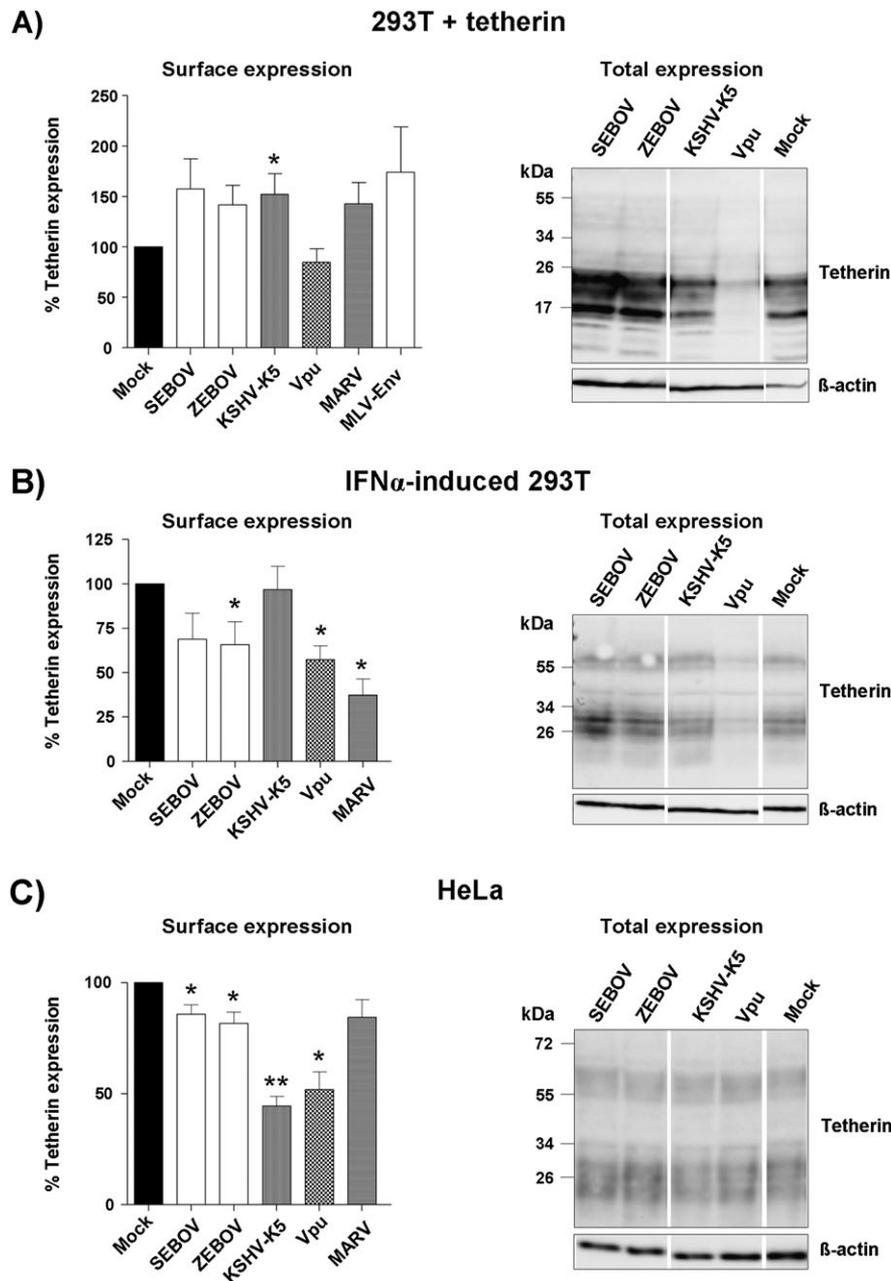
Figure 4. The Ebola virus glycoprotein does not interfere with robust tetherin expression. *A*, Plasmids encoding for the GPs of the indicated filoviruses, KSVH-K5, or Vpu and a tetherin expression plasmid were cotransfected into 293T cells. As control, the cells were transfected with tetherin expression plasmid and empty vector. At 48 hours posttransfection, surface expression of tetherin was determined by FACS (*left panel*) and tetherin levels in cell lysates were determined by Western blot (*right panel*). The FACS data represent the average of 7 independent experiments (4 for MARV-GP, 11 for MLV envelope protein); error bars indicate SEM. *B*, The 293T cells were treated with IFN-α to induce tetherin expression and transfected with the plasmids encoding Vpu, KSHV-K5, or the GPs of the indicated filoviruses. Tetherin levels on the cell surface (*left panel*) and in cell lysates (*right panel*) were determined by FACS analysis and Western blot, respectively. The FACS data represent the average of 6 independent experiments (4 for MARV-GP); error bars indicate SEM. *C*, HeLa cells, which express endogenous tetherin, were transfected with plasmids encoding Vpu, KSHV-K5, or the GPs of the indicated filoviruses, and tetherin levels on the cell surface (*left panel*) and in cell lysates (*right panel*) were determined by FACS analysis and Western blot, respectively. The FACS data represent the average of 8 independent experiments (3 for MARV-GP); error bars indicate SEM. For all FACS experiments, geometric mean channel fluorescence was determined, background corrected (isotype control for all cell lines tested), and signals measured for tetherin expression in the absence of Vpu or a Vpu-like factor were set as 100%. In the absence of viral protein expression, the following geometric mean channel fluorescence was measured for the cell lines tested: HeLa: 175 ± 58; 293T + tetherin: 48 ± 18; 293T + IFNα: 32 ± 13. Statistical significance was assessed using 2-tailed Student *t* test for paired samples. *P* values below .05 were considered significant (*); *P* values below .001 were considered highly statistically significant (**).
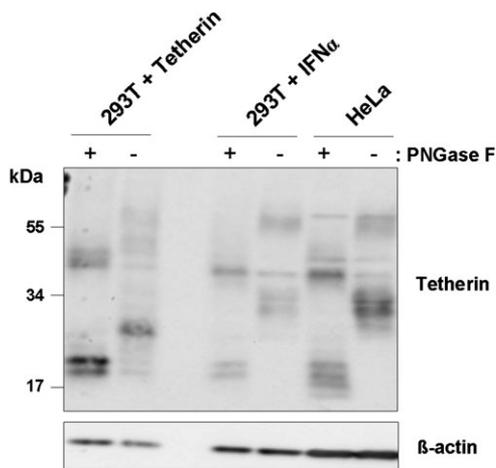
Figure 5. Glycosylation of tetherin is cell type–dependent. The 293T cells transfected with a tetherin expression plasmid, 293T cells induced by IFNα to express tetherin, and HeLa (expressing endogenous tetherin) were lysed, the lysates treated with PNGase F or mock treated, and the presence of tetherin analyzed by Western blot. Detection of β-actin levels served as loading control.

a scenario, a FRET signal indicative of an interaction between GP2 and tetherin was only obtained with a GP2 harboring the fluorophore at its N-terminus. Alternatively, EBOV-GP–induced relocalization of tetherin might be responsible for tetherin antagonism. Thus, tetherin localizes to lipid raft microdomains in the plasma membrane [15], which are also the location of HIV and EBOV budding [47, 48], raising the possibility that EBOV-GP blocks tetherin's antiviral activity by interfering with lipid raft localization of this protein or by redirecting the budding complex into certain lipid rafts in which tetherin is not present.

The ability of MARV-GP and KSHV-K5 to reduce cell surface expression of tetherin was cell type–dependent, and a similar observation was previously made for Vpu [35, 38]. The determinants underlying cell type dependence are at present unclear but might encompass expression differences or the need for a so far unidentified, differentially expressed cofactor for tetherin downregulation. We found that N-linked glycosylation of tetherin was dependent on the source of cellular tetherin, a finding that confirms and extends a previous report [16]. While the integrity of the glycosylation signals seems to be largely dispensable for antiviral activity in transfected cells [16, 49], it can be speculated that a certain tetherin glycosylation pattern might not be compatible with optimal transport of the protein to sites of viral budding and/or with optimal recognition of tetherin by viral defense proteins. It should be noted, however, that glycosylation differences are unlikely to account for the differential interference of viral proteins with tetherin surface expression in HeLa and IFNα-treated 293T cells (Figure 4), since similar tetherin glycospecies were detected in these cells lines.

The counteraction of tetherin by Vpu depends on the interaction of the transmembrane domains of both proteins [50].
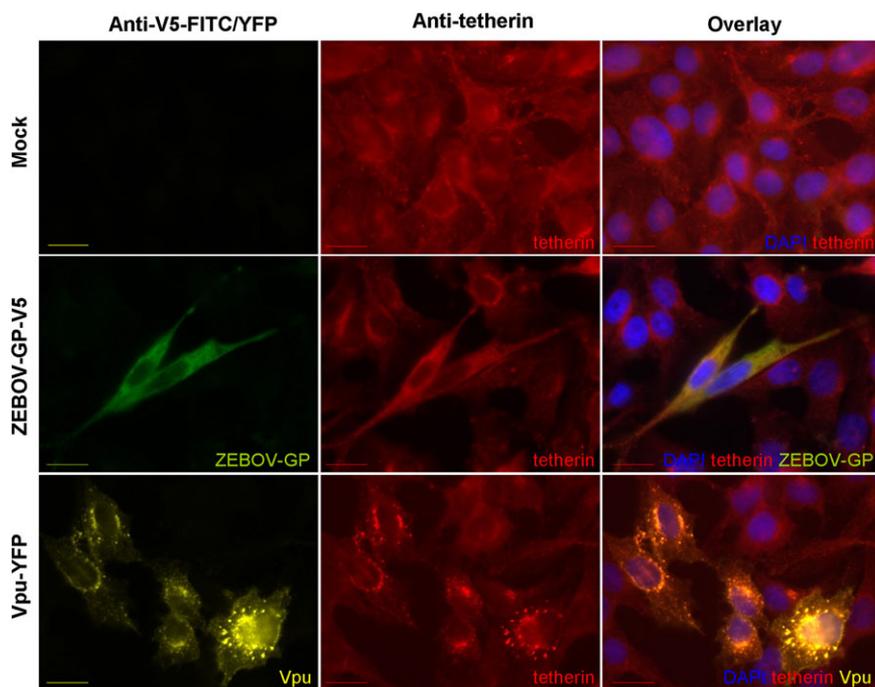

Figure 6. Vpu but not the Ebola virus glycoprotein relocalizes tetherin into intracellular compartments. HeLa cells, which express endogenous tetherin, were transfected with plasmids encoding ZEBOV-GP (containing a C-terminal V5 tag) or Vpu fused to YFP or control transfected with empty vector, and expression of tetherin, ZEBOV-GP, and Vpu analyzed by immunofluorescence. The bar indicates a distance of 20 μm.

An interaction between ZEBOV-GP and tetherin has also been demonstrated [8], but the domain(s) in ZEBOV-GP, which bind to tetherin, are unknown. Our results indicate that the transmembrane unit of ZEBOV-GP, GP2, interacts with tetherin. Isolated GP2 was able to relocalize tetherin, while the entire ZEBOV-GP was not, indicating that GP1 arrests GP-tetherin complexes at the plasma membrane. A role for GP2 in tetherin interactions is perhaps not unexpected since the GP2 equivalent of the envelope protein of HIV-2, specifically its cytoplasmic tail, is required for efficient tetherin counteraction, although specificity for tetherin seems to be determined by the extracellular portion of the envelope (Env) [11]. The tetherin-binding domain in GP2 is at present unknown. Our preliminary data suggest that the deletion of the cytoplasmic tails of EBOV-GP and MARV-GP is compatible with tetherin counteraction (data not shown). Future efforts to identify the tetherin-binding domain in GP2 should therefore focus on the role of the transmembrane domain and the extracellular portion of GP2 in tetherin binding and counteraction.

Supplementary Data

Supplementary Data are available at *The Journal of Infectious Diseases* online.

Funding

Acknowledgments

References

1. Neil SJ, Zang T, Bieniasz PD. Tetherin inhibits retrovirus release and is antagonized by HIV-1 Vpu. Nature 2008; 451:425–30.
2. Van Damme N, Goff D, Katsura C, et al. The interferon-induced protein BST-2 restricts HIV-1 release and is downregulated from the cell surface by the viral Vpu protein. Cell Host Microbe 2008; 3: 245–52.
3. Sauter D, Specht A, Kirchhoff F. Tetherin: holding on and letting go. Cell 2010; 141:392–8.
4. Warfield KL, Deal EM, Bavari S. Filovirus infections. J Am Vet Med Assoc 2009; 234:1130–9.
5. Harty RN, Brown ME, Wang G, Huibregtse J, Hayes FP. A PPxY motif within the VP40 protein of Ebola virus interacts physically and functionally with a ubiquitin ligase: implications for filovirus budding. Proc Natl Acad Sci USA 2000; 97:13871–6.
6. Jouvenet N, Neil SJ, Zhadina M, et al. Broad-spectrum inhibition of retroviral and filoviral particle release by tetherin. J Virol 2009; 83: 1837–44.
7. Neil SJ, Sandrin V, Sundquist WI, Bieniasz PD. An interferon-alpha-induced tethering mechanism inhibits HIV-1 and Ebola virus particle release but is counteracted by the HIV-1 Vpu protein. Cell Host Microbe 2007; 2:193–203.
8. Kaletsky RL, Francica JR, Agrawal-Gamse C, Bates P. Tetherin-mediated restriction of filovirus budding is antagonized by the Ebola glycoprotein. Proc Natl Acad Sci USA 2009; 106:2886–91.
9. Gupta RK, Mlcochova P, Pelchen-Matthews A, et al. Simian immunodeficiency virus envelope glycoprotein counteracts tetherin/BST-2/CD317 by intracellular sequestration. Proc Natl Acad Sci USA 2009; 106:20889–94.
10. Jia B, Serra-Moreno R, Neidermyer W, et al. Species-specific activity of SIV Nef and HIV-1 Vpu in overcoming restriction by tetherin/BST2. PLoS Pathog 2009; 5:e1000429.
11. Le Tortorec A, Neil SJ. Antagonism to and intracellular sequestration of human tetherin by the human immunodeficiency virus type 2 envelope glycoprotein. J Virol 2009; 83:11966–78.
12. Zhang F, Wilson SJ, Landford WC, et al. Nef proteins from simian immunodeficiency viruses are tetherin antagonists. Cell Host Microbe 2009; 6:54–67.
13. Pardieu C, Vigan R, Wilson SJ, et al. The RING-CH ligase K5 antagonizes restriction of KSHV and HIV-1 particle release by mediating ubiquitin-dependent endosomal degradation of tetherin. PLoS Pathog 2010; 6:e1000843.
14. Sakuma T, Noda T, Urata S, Kawaoka Y, Yasuda J. Inhibition of Lassa and Marburg virus production by tetherin. J Virol 2009; 83:2382–5.
15. Kupzig S, Korolchuk V, Rollason R, Sugden A, Wilde A, Banting G. Bst-2/HM1.24 is a raft-associated apical membrane protein with an unusual topology. Traffic 2003; 4:694–709.
16. Perez-Caballero D, Zang T, Ebrahimi A, et al. Tetherin inhibits HIV-1 release by directly tethering virions to cells. Cell 2009; 139:499–511.
17. Fitzpatrick K, Skasko M, Deerinck TJ, Crum J, Ellisman MH, Guatelli J. Direct restriction of virus release and incorporation of the interferon-induced protein BST-2 into HIV-1 particles. PLoS Pathog 2010; 6:e1000701.
18. Hammonds J, Wang JJ, Yi H, Spearman P. Immunoelectron microscopic evidence for tetherin/BST2 as the physical bridge between HIV-1 virions and the plasma membrane. PLoS Pathog 2010; 6:e1000749.
19. Hinz A, Miguet N, Natrajan G, et al. Structural basis of HIV-1 tethering to membranes by the BST-2/tetherin ectodomain. Cell Host Microbe 2010; 7:314–23.
20. Dube M, Roy BB, Guiot-Guillain P, et al. Antagonism of tetherin restriction of HIV-1 release by Vpu involves binding and sequestration of the restriction factor in a perinuclear compartment. PLoS Pathog 2010; 6:e1000856.
21. Goffinet C, Homann S, Ambiel I, et al. Antagonism of CD317 restriction of human immunodeficiency virus type 1 (HIV-1) particle release and depletion of CD317 are separable activities of HIV-1 Vpu. J Virol 2010; 84:4089–94.
22. Mangeat B, Gers-Huber G, Lehmann M, Zufferey M, Luban J, Piguet V. HIV-1 Vpu neutralizes the antiviral factor tetherin/BST-2 by binding it and directing its beta-TrCP2-dependent degradation. PLoS Pathog 2009; 5:e1000574.
23. Douglas JL, Viswanathan K, McCarroll MN, Gustin JK, Fruh K, Moses AV. Vpu directs the degradation of the human immunodeficiency virus restriction factor BST-2/tetherin via a βTrCP-dependent mechanism. J Virol 2009; 83:7931–47.
24. Jiang D, Guo H, Xu C, et al. Identification of three interferon-inducible cellular enzymes that inhibit the replication of hepatitis C virus. J Virol 2008; 82:1665–78.
25. Gao F, Li Y, Decker JM, et al. Codon usage optimization of HIV type 1 subtype C gag, pol, env, and nef genes: in vitro expression and immune

responses in DNA-vaccinated mice. AIDS Res Hum Retrov **2003**; 19:817–23.

26. Nguyen KL, llano M, Akari H, et al. Codon optimization of the HIV-1 vpu and vif genes stabilizes their mRNA and allows for highly efficient Rev-independent expression. Virology **2004**; 319:163–75.

27. Marzi A, Gramberg T, Simmons G, et al. DC-SIGN and DC-SIGNR interact with the glycoprotein of Marburg virus and the S protein of severe acute respiratory syndrome coronavirus. J Virol **2004**; 78:12090–5.

28. Marzi A, Akhavan A, Simmons G, et al. The signal peptide of the Ebolavirus glycoprotein influences interaction with the cellular lectins DC-SIGN and DC-SIGNR. J Virol **2006**; 80:6305–17.

29. Sander G, Konrad A, Thurau M, et al. Intracellular localization map of human herpesvirus 8 proteins. J Virol **2008**; 82:1908–22.

30. McNatt MW, Zang T, Hatziioannou T, et al. Species-specific activity of HIV-1 Vpu and positive selection of tetherin transmembrane domain variants. PLoS Pathog **2009**; 5:e1000300.

31. Sauter D, Schindler M, Specht A, et al. Tetherin-driven adaptation of Vpu and Nef function and the evolution of pandemic and non-pandemic HIV-1 strains. Cell Host Microbe **2009**; 6:409–21.

32. Banning C, Votteler J, Hoffmann D, et al. A flow cytometry-based FRET assay to identify and analyse protein-protein interactions in living cells. PLoS One **2010**; 5:e9344.

33. Kühl A, Munch J, Sauter D, et al. Calcium-modulating cyclophilin ligand does not restrict retrovirus release. Nat Med **2010**; 16:155–6.

34. Kawai S, Yoshimura Y, Iida S, et al. Antitumor activity of humanized monoclonal antibody against HM1.24 antigen in human myeloma xenograft models. Oncol Rep **2006**; 15:361–7.

35. Miyagi E, Andrew AJ, Kao S, Strebel K. Vpu enhances HIV-1 virus release in the absence of Bst-2 cell surface down-modulation and intracellular depletion. Proc Natl Acad Sci USA **2009**; 106:2868–73.

36. Bermejo M, Rodriguez-Teijeiro JD, Illera G, Barroso A, Vila C, Walsh PD. Ebola outbreak killed 5000 gorillas. Science **2006**; 314:1564.

37. Leroy EM, Rouquet P, Formenty P, et al. Multiple Ebola virus transmission events and rapid decline of central African wildlife. Science **2004**; 303:387–90.

38. Sato K, Yamamoto SP, Misawa N, Yoshida T, Miyazawa T, Koyanagi Y. Comparative study on the effect of human BST-2/tetherin on HIV-1 release in cells of various species. Retrovirology **2009**; 6:53.

39. Schindler M, Rajan D, Banning C, et al. Vpu serine 52 dependent counteraction of tetherin is required for HIV-1 replication in macrophages, but not in ex vivo human lymphoid tissue. Retrovirology **2010**; 7:1.

40. Mansouri M, Viswanathan K, Douglas JL, et al. Molecular mechanism of BST2/tetherin downregulation by K5/MIR2 of Kaposi's sarcoma-associated herpesvirus. J Virol **2009**; 83:9672–81.

41. Goffinet C, Schmidt S, Kern C, Oberbremer L, Keppler OT. Endogenous CD317/tetherin limits replication of HIV-1 and MLV in rodent cells and is resistant to antagonists from primate viruses. J Virol **2010**; 84:11374–84.

42. Mitchell RS, Katsura C, Skasko MA, et al. Vpu antagonizes BST-2-mediated restriction of HIV-1 release via beta-TrCP and endolysosomal trafficking. PLoS Pathog **2009**; 5:e1000450.

43. Licata JM, Johnson RF, Han Z, Harty RN. Contribution of Ebola virus glycoprotein, nucleoprotein, and VP24 to budding of VP40 virus-like particles. J Virol **2004**; 78:7344–51.

44. Radoshitzky SR, Dong L, Chi X, et al. Infectious Lassa virus, but not filoviruses, is restricted by BST-2/tetherin. J Virol **2010**; 84: 10569–80.

45. Goffinet C, Allespach I, Homann S, et al. HIV-1 antagonism of CD317 is species specific and involves Vpu-mediated proteasomal degradation of the restriction factor. Cell Host Microbe **2009**; 5:285–97.

46. Lopez LA, Yang SJ, Hauser H, et al. Ebola virus glycoprotein counteracts BST-2/tetherin restriction in a sequence-independent manner that does not require tetherin surface removal. J Virol **2010**; 84:7243–55.

47. Bavari S, Bosio CM, Wiegand E, et al. Lipid raft microdomains: a gateway for compartmentalized trafficking of Ebola and Marburg viruses. J Exp Med **2002**; 195:593–602.

48. Nguyen DH, Hildreth JE. Evidence for budding of human immunodeficiency virus type 1 selectively from glycolipid-enriched membrane lipid rafts. J Virol **2000**; 74:3264–72.

49. Andrew AJ, Miyagi E, Kao S, Strebel K. The formation of cysteine-linked dimers of BST-2/tetherin is important for inhibition of HIV-1 virus release but not for sensitivity to Vpu. Retrovirology **2009**; 6:80.

50. Iwabu Y, Fujita H, Kinomoto M, et al. HIV-1 accessory protein Vpu internalizes cell-surface BST-2/tetherin through transmembrane interactions leading to lysosomes. J Biol Chem **2009**; 284:35060–72.